[Article] www.whxb.pku.edu.cn

邻溴甲苯在 234 和 267 nm 的光解动力学

曹振洲 张昌华 王艳梅 张 锋 华林强 张 冰*

(中国科学院武汉物理与数学研究所, 波谱与原子分子物理国家重点实验室, 武汉 430071;
中国科学院研究生院, 北京 100049)

摘要: 利用离子速度影像技术结合共振增强多光子电离(REMPI)技术, 研究了邻溴甲苯在 234 和 267 nm 激光作用下的光解机理. 平动能分布表明, 基态 Br($^2P_{3/2}$)和自旋轨道激发态 Br*($^2P_{1/2}$)产生于两个解离通道: 快通道和慢通道.快通道的各向异性参数在 234 nm 分别为 1.15(Br)和 0.55(Br*), 在 267 nm 分别为 0.90(Br)和 0.60(Br*). 慢通道的各向异性参数在 234 nm 分别为 0.12(Br)和 0.14(Br*), 在 267 nm 分别为 0.11(Br)和 0.10(Br*). 源自于慢通道的 Br 和 Br*碎片的各向异性弱于快通道. Br($^2P_{3/2}$)的相对量子产率 Φ(Br)在 234 nm 为 0.67, 在 267 nm 为 0.70. 邻溴甲苯在 234 和 267 nm 光解主要产生基态产物 Br($^2P_{3/2}$). 快通道产生于(π, π^*)束缚单重态被激发, 随后通过排斥性(n, σ^*)态的预解离. 慢通道各向异性参数接近零, 由此证实慢通道来源于单重激发态内转换到高振动基态而引发的热解离.

关键词: 离子速度影像; 光解离; 邻溴甲苯
中图分类号: O644

Photodissociation Dynamics of *o*-Bromotoluene at 234 and 267 nm

CAO Zhen-Zhou ZHANG Chang-Hua WANG Yan-Mei ZHANG Feng
HUA Lin-Qiang ZHANG Bing*

(*State Key Laboratory of Magnetic Resonance and Atomic and Molecular Physics, Wuhan Institute of Physics and Mathematics, Chinese Academy of Sciences, Wuhan 430071, P. R. China*; *Graduate School of the Chinese Academy of Sciences, Beijing 100049, P. R. China*)

Abstract: The photodissociation of *o*-bromotoluene was studied at 234 and 267 nm using velocity map imaging combined with a resonance-enhanced multiphoton ionization (REMPI) technique. Translational energy distributions suggested that ground state Br($^2P_{3/2}$) and spin-orbit excited state Br*($^2P_{1/2}$) fragments were all generated *via* two dissociation channels: a fast channel and a slow channel. The anisotropy parameters of the fast channels were determined to be 1.15 (Br) and 0.55 (Br*) at 234 nm, 0.90 (Br) and 0.60 (Br*) at 267 nm. The anisotropy parameters of the slow channels were 0.12 (Br) and 0.14 (Br*) at 234 nm, 0.11 (Br) and 0.10 (Br*) at 267 nm. The Br and Br* fragments of the slow channel were less anisotropic than those of the fast channel. The total relative quantum yields of Br (Φ(Br)) were 0.67 at 234 nm and 0.70 at 267 nm. Ground state Br($^2P_{3/2}$) was the main product from the photolysis of *o*-bromotoluene at 234 and 267 nm. We propose that the fast channel originates from excitation of bound excited singlet (π, π^*) states followed by predissociation along repulsive (n, σ^*) states. The anisotropy parameters of the slow channels were close to zero indicating a hot dissociation mechanism on a highly vibrational ground state followed the internal conversion of the excited singlet state.

Key Words: Ion velocity imaging; Photodissociation; *o*-Bromotoluene

Photochemistry of halogenated molecules including alkyl and aryl halides has received much attention, not only for their ex-

Received: October 7, 2008; Revised: November 25, 2008; Published on Web: December 31, 2008.
*Corresponding author. Email: BZhang@wipm.ac.cn; Tel: +8627-87197441; Fax: +8627-87198576.
国家自然科学基金(10534010, 20673140)资助项目

treme importance to the environmental protection but also from a fundamental viewpoint where the understanding of the detailed dynamics is of interest. For alkyl halides, UV irradiation may lead to transition from a nonbonding electron of the halogen atom to the antibonding orbital of the C—X bond (X denotes halogens), thereby rapidly causing bond fission[1−10]. In contrast, the photodissociation of aryl halides are more complicated because more electronic states might be involved to make multiple dissociation channels probable[11−20]. For instance, El-sayed *et al*.[15] proposed that iodobenzene is excited to two states simultaneously: one is a repulsive (n, σ^*) excitation in the C—I bond and the other is a bound triplet (π, π^*) excitation in benzene-ring, and thus the dissociation is through two channels as well: a direct-mode due to the C—I bond repulsion and a complex-mode due to the electronic predissociation. The dissociation rates and channels of aryl halides depend on the type of halogen, substituents on the benzene ring and related positions, and excitation wavelengths. Among the aryl halides, the simplest type of monohalobenzenes including chlorobenzene[21], bromobenzene[19,22], iodoben zene[11,12,15,23−25], and fluorobenzene[26−28] have been widely studied. When the substituents on the benzene ring increase, their nature and positions may cause substantial impact on the photodissociation behavior[13,14,16,17,20,29−32]. For instance, by using femtosecond pump-probe spectroscopy, Davidsson′s group[18] investigated photodissociation dynamics of *o*-, *m*-, and *p*-dibromobenzene and 1,3,5-tribromobenzene at 266 nm. The common channel for all these molecules was ascribed to predissociation *via* intersystem crossing (ISC). The second dissociation channel, observed in *o*- and *m*-dibromobenzene, was opened up because of the lowering of symmetry from C_{2v} to C_s.

Considering the substitute effects on dissociation mechanism, Ichimura *et al*.[14] have suggested that photodecomposition of the C—Cl bond in chlorobenzene may take place through three different channels, i.e., a direct dissociation channel, a channel *via* vibrational excited triplet levels, and a channel *via* highly excited vibrational levels of the ground electronic state. The methyl substituent enhances the route involving ISC by increasing the rotational levels. The effect of methyl group substitution was also studied for *o*-, *m*-, and *p*-bromotoluene[31,32]. The substituents affect the coupling strength between different states, causing competition among these dissociation channels.

The photodissociations of *o*-, *m*-, and *p*-bromotoluene were investigated by *ab initio* calculations[33]. The possible photodissociation mechanisms at 266 and 193 nm were clarified by calculated potential energy curves, vertical excitation energies, and oscillator strengths of low-lying states, using multistate second order multiconfigurational perturbation theory (MS-CASPT2). From potential energy curves, the predissociation can be easily understood.

Photofragment translational spectroscopy (PTS) has been widely used to study photodissociation dynamics of aryl halides[11−15,19-21,24,25,29,31,32]. To the best of our knowledge, velocity imaging detection coupled with REMPI has been seldom applied to the investigation of photodissociation of aryl halides except for iodobenzene and bromofluorobenzene[34−37]. To clarify the photodissociation mechanisms of ringlike molecules, we have studied dissociation mechanisms of 2-bromothiophene and 3-bromothiophene at 267 nm, and 1-bromocyclohexane at 234 nm recently[38,39]. Intersystem crossing mechanism is also proposed. In this work, the photodissociation dynamics of *o*-bromotoluene was investigated employing the velocity map imaging technique coupled with REMPI at 234 and 267 nm. In the present study, the angular and translational energy distributions of both Br* and Br fragments were obtained. The [Br*]/[Br] branching ratio at 234 and 267 nm was measured. The possible dissociation mechanism was analyzed.

1 Experimental methods

The experimental setup has been described in detail elsewhere[40]. Briefly, it consisted of a homebuilt time-of-flight (TOF) mass spectrometer and a two-dimensional (2D) position sensitive detector. The vacuum chamber was divided into two stages by a 1 mm skimmer, and was maintained to a background pressure of 4×10^{-6} Pa. Sample gas, typically 5% diluted in helium, were expanded at a backing pressure of 1×10^5 Pa through a pulsed valve (Parker, General Valve) and intersected with a linearly polarized tunable UV laser in the reaction region which was located in the second stage of the vacuum chamber. The UV laser was the frequency-doubled output of a dye laser system (Lambda Physik, ScanMate 2E OG), which was pumped by 355 nm light from the third harmonic of a Nd:YAG laser (Quantel, YAG980), and used for both dissociation and state-selective ionization of bromine atoms. The polarization vector of the UV laser, which was set parallel to the detector plane and the laser was focused perpendicularly onto the ionization zone using a 250 mm focal length lens.

The bromine-atom fragments were ionized by the (2+1) REMPI[41]. The ground state of bromine was probed *via* $5p(^4P^0_{3/2})\leftarrow 4p^5(^2P^0_{3/2})$ transition at 266.55 nm and the excited state was probed *via* $5p(^4S^0_{3/2})\leftarrow 4p^5(^2P^0_{1/2})$ transition at 266.61 nm. In the 234 nm region the Br and Br* atoms were ionized *via* $6p(^4P^0_{3/2})\leftarrow 4p^5(^2P^0_{3/2})$ and *via* $6p(^2S^0_{1/2})\leftarrow 4p^5(^2P^0_{1/2})$ transition at 233.62 and 233.95 nm. The generated ions were extracted and accelerated by the electrostatic immersion lens and projected onto a 2D detector composed with a microchannel plate (MCP)/phosphor screen and a charge-coupled device (CCD) camera. The REMPI-TOF mass spectra were acquired using a photomultiplier tube. The velocity map imaging was allowed by the specially designed electrostatic immersion lens. A high voltage pulse with 1 μs duration was applied to MCP to separate the bromine ion signal from those of scattered laser light and background ions with different masses. The typical energy of the laser used in the experiments was kept at 200−300 μJ per pulse to minimize the space charge effect between the ionized fragments. *o*-Bromotoluene (>95%) was used without further purification.

2 Results

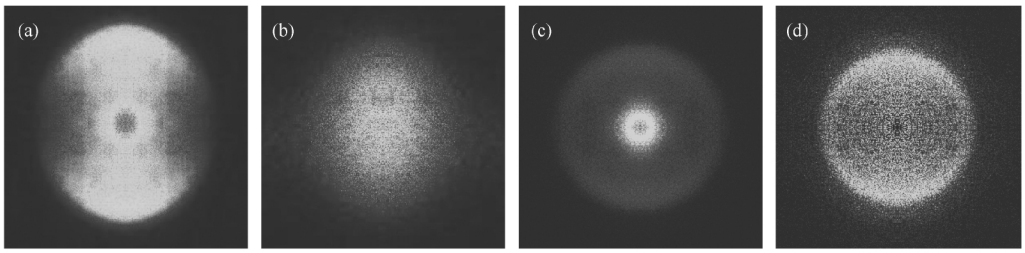

Fig.1 Raw ion images of Br and Br* fragments from the photodissociation of *o*-bromotoluene at 234 and 267 nm

The laser is linearly polarized along the vertical direction. (a) Br at 234 nm, (b) Br* at 234 nm, (c) Br at 267 nm, (d) Br* at 267 nm

2.1 Translational energy distributions of photofragments

The raw ion images of Br and Br* resulting from photodissociation of *o*-bromofluorobenzene at 234 and 267 nm are shown in Fig.1. From Fig.1(a, c), it can be seen that the distributions of fragments consist of two components. Image at 234 nm is more anisotropic than that at 267 nm. The Br* fragment ions (Fig.1(b, d)) show large differences: the image at 267 nm displays anisotropic angular distributions along the polarization of the photolysis laser, whereas the image at 234 nm is a round "cake" in which no intrinsical structure is presented. These facts indicate that the configurations of the excited states are so complicated that the change of the photon energy will lead to the large difference in images of the photoproducts Br and Br*.

Each image is accumulated over 30000 laser shots, and the background is removed by subtracting a reference image collected at offresonance wavelength under otherwise the same conditions. The laser wavelength was scanned back and forth within the range of Doppler broadening to cover all the velocity components of the selected fragments. The scan range (0.01 nm) is very small; the effect of wavelength change to photodissociation can be neglected. Each raw image is 2D projection of the three-dimensional (3D) speed and angular distributions with cylindrical symmetry around the polarization axis of the photolyzing laser. According to the method of inverse Abel transformation, the corresponding 3D spatial distributions of the fragments are reconstructed and displayed in Fig.2.

The speed distribution $P(v)$ can be extracted by integrating the reconstructed 3D speed distribution over all angles at each speed. For *o*-bromotoluene, the center-of-mass translational energy distribution $P(E_T)$ may be obtained by converting the speed distribution using the following equations:

$$P(E_T)=P(v)\frac{dv}{dE_T} \tag{1}$$

$$E_T=\frac{1}{2}(m_{Br}+m_{C_7H_7})\times(\frac{m_{Br}}{m_{C_7H_7}})\times v_{Br}^2 \tag{2}$$

where E_T is the total translational energy, m_X is the mass of X (X=Br or C_7H_7), and v_{Br} is the velocity of the bromine fragment. The available energy E_{avl} for the dissociation process is evaluated by

$$E_{avl}=h\nu-E_{dis}+E_{int} \tag{3}$$

$$E_{int}=E_{avl}-E_T-E_{ele} \tag{4}$$

where $h\nu$ is the photon energy, E_{ele} is the electronic energy of the bromine atom, which is 0 kJ·mol^{-1} for Br and 44 kJ·mol^{-1} for Br*. E_{dis} denotes the dissociation energy of the C—Br bond, which is 343 kJ·mol^{-1} [42,43]. E_{int} is the internal energy of the parent molecule. Compared with $h\nu$ and E_{dis}, E_{int} can be neglected since a supersonic molecular beam was used in our experiment. The fraction of the translational energy deposition (f_{tr}), defined as a ratio of the average translational energy to the available energy, can be determined by

$$f_{tr}=\langle E_T\rangle/E_{avl} \tag{5}$$

Fig.3 shows the center-of-mass translational energy distributions of Br and Br* photofragmentation from *o*-bromotoluene. Each distribution of Br and Br* can be fitted by two Gaussian curves. The first distribution is the slow component of dissociation, and the second distribution is the fast component of dissociation. For the slow channel of 234 nm excitation, the total average translational energy $\langle E_T\rangle$ are 23.7 kJ·mol^{-1} (Br) and 16.2 kJ·mol^{-1} (Br*), which are about 14% and 13% of the available energy, and there are about 86% and 87% of the available energy partitioned into the fragment internal energy. For the fast channel of 234 nm excitation, the values of $\langle E_T\rangle$ are 69.3 kJ·mol^{-1} (Br) and 52.2 kJ·mol^{-1} (Br*), which are about 41% and 42%

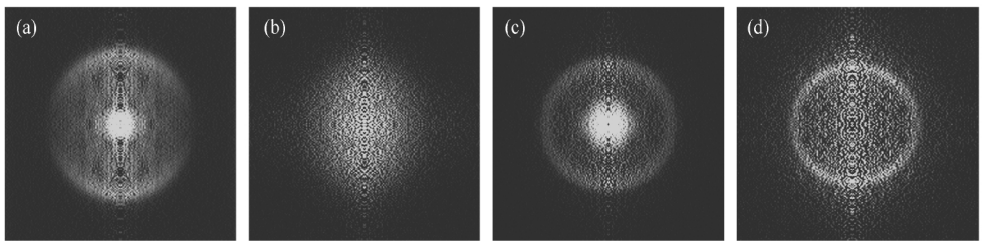

Fig.2 Inverse Abel-transformed ion images of Br and Br* fragments from the photodissociation of *o*-bromotoluene at 234 and 267 nm

The laser is linearly polarized along the vertical direction. (a) Br at 234 nm, (b) Br* at 234 nm, (c) Br at 267 nm, (d) Br* at 267 nm

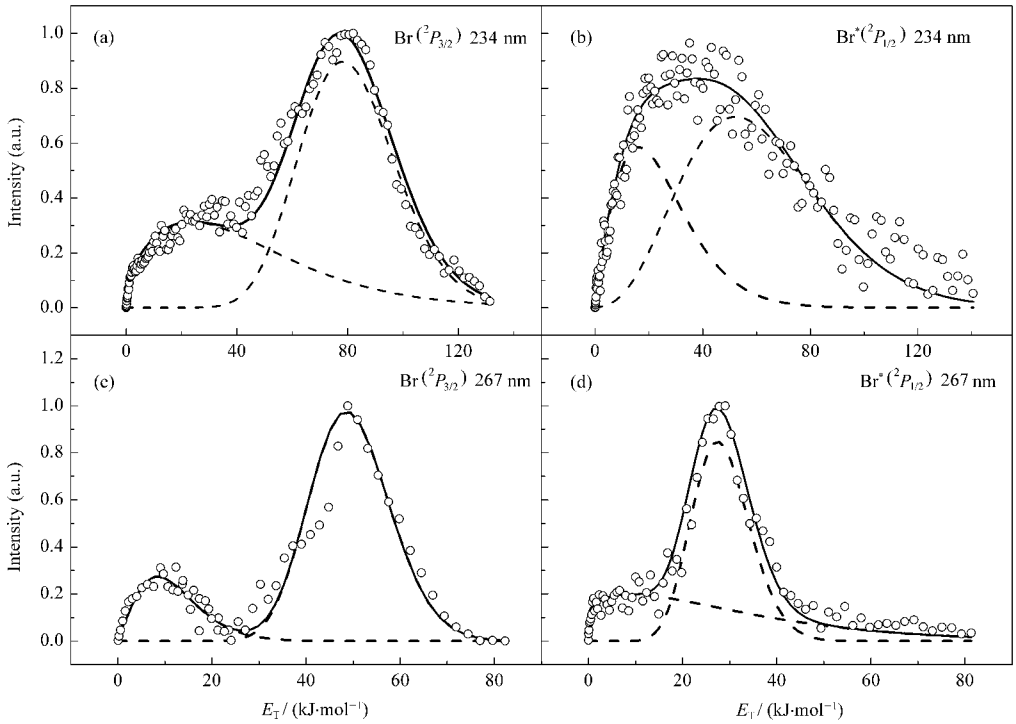

Fig.3 Total translational energy distributions of the Br($^2P_{3/2}$) and Br*($^2P_{1/2}$) fragments produced from photodissociation of *o*-bromotoluene at 234 and 267 nm

○ experimental data, —— fitting data, –– fitting components

of the available energy. The available energy partitioned into the fragment internal energy decreases. The f_{tr} values of 267 nm excitation are 0.08 (Br) and 0.14 (Br*) for the slow channel, 0.46 (Br) and 0.45 (Br*) for the fast channel. Such a partition of the available energy is similar to the results of Han and coworkers[20]. For *o*-bromotoluene photodissociation at 266 nm, the average translation energies for the two dissociation channels are about 9% and 44% of the available energy, respectively. The translational energy and available energy partitions are listed in Table 1.

2.2 Angular distributions of the photofragments

In a photodissociation process, angular distribution ($I(\theta)$) of the fragment can be obtained by integrating the reconstructed 3D spatial distribution over a proper range of speed at each angle. It may be characterized by an anisotropy parameter (β) as expressed by[44,45]

$$I(\theta)=\frac{1}{4\pi}[1+\beta P_2(\cos\theta)] \quad (6)$$

where β is limited between 2 and −1, and $P_2(\cos\theta)$ is the second order Legendre polynomial. θ is the angle between the laser polarization direction and the recoil velocity of fragments. The β values can be obtained by least-squares fit to the angular distributions which are shown in Fig.4.

In this manner, the β values determined from the Br and Br* images at 234 and 267 nm photodissociation are listed in Table 1. For the photodissocation of *o*-bromotoluene, β(Br) and β(Br*) of the lower speed components are very small, indicating that the related dissociation channels are slow enough to produce the isotropic fragments. In contrast, β(Br) and β(Br*) of the higher speed components are larger; the anisotropic feature of the fragments indicates that the dissociation rate is faster than the molec-

Table 1 Relative quantum yields, anisotropy parameters, and energies of bromine fragments

λ/nm	State	Channel	$h\nu$/(kJ·mol^{-1})	E_{avl}/(kJ·mol^{-1})	v/(m·s^{-1})	$\langle E_T\rangle$/(kJ·mol^{-1})	f_{tr}	Φ	β
233.62	Br($^2P^0_{3/2}$)	1st (slow)	512.1	169.1	561.7	23.7	0.14	0.32	0.12
		2nd (fast)		169.1	960.5	69.3	0.41	0.35	1.15
233.95	Br*($^2P^0_{1/2}$)	1st (slow)	511.4	124.4	464.4	16.2	0.13	0.13	0.14
		2nd (fast)		124.4	833.6	52.2	0.42	0.20	0.55
266.55	Br($^2P^0_{3/2}$)	1st (slow)	448.8	105.7	336.4	8.5	0.08	0.23	0.11
		2nd (fast)		105.7	804.4	48.6	0.46	0.47	0.90
266.61	Br*($^2P^0_{1/2}$)	1st (slow)	448.7	61.6	338.4	8.6	0.14	0.17	0.10
		2nd (fast)		61.6	607.3	27.7	0.45	0.13	0.60

λ: wavelength, $h\nu$: absorbed photon energy, E_{avl}: available energy, v: velocity of the bromine fragment, $\langle E_T\rangle$: total average translational energy, f_{tr}: fraction of the translational energy deposition, Φ: relative quantum yield, β: anisotropic parameter

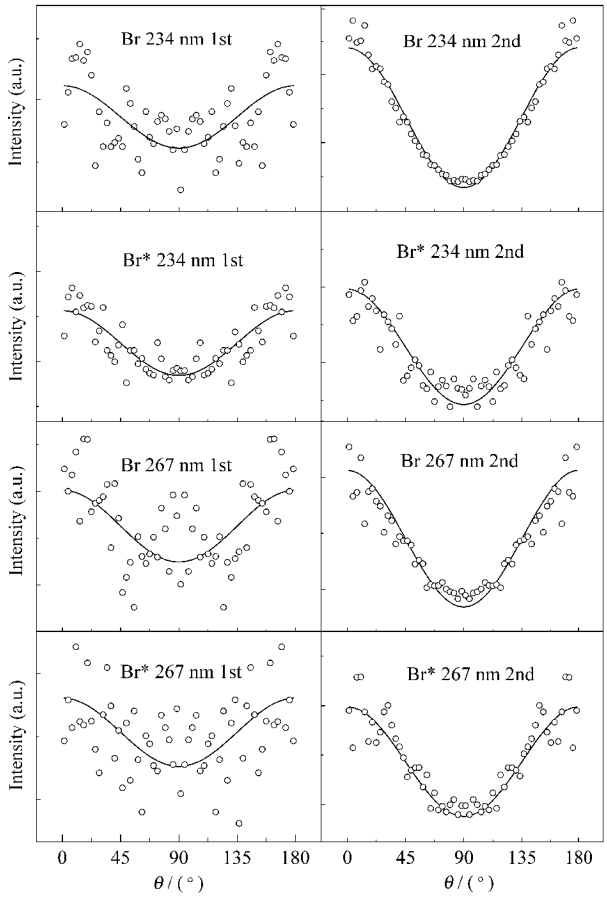

Fig.4 Photoion angular distributions for each channel

The circles present the experimental data. The solid lines are the least-squares fits of the experimental angular distributions.

ular rotation period.

2.3 Relative quantum yields of *o*-bromotoluene

The obtained bromine ion signal is related to its state population by

$$\frac{N(\mathrm{Br}^*)}{N(\mathrm{Br})}=k\frac{S(\mathrm{Br}^*)}{S(\mathrm{Br})} \tag{7}$$

where $N(\mathrm{Br}^*)$ and $N(\mathrm{Br})$ are the numbers of Br^* and Br fragments; $S(\mathrm{Br}^*)$ and $S(\mathrm{Br})$ are the measured ion intensities. The factor k is associated with the transition probability ratios in REMPI and the related instrument factors. It can be evaluated by performing a calibration experiment of Br_2 photolysis under the same conditions. The k value was thus determined to be 0.69 and 0.81 in the 234 and 267 nm photolysis of Br_2. The relative quantum yields $\Phi(\mathrm{Br}^*)$ and $\Phi(\mathrm{Br})$ can be readily obtained by the following equations:

$$\Phi(\mathrm{Br}^*)=\frac{N(\mathrm{Br}^*)}{N(\mathrm{Br})+N(\mathrm{Br}^*)} \tag{8}$$

$$\Phi(\mathrm{Br})=1-\Phi(\mathrm{Br}^*) \tag{9}$$

The results are listed in Table 1. The total relative quantum yields $\Phi(\mathrm{Br}^*)$ were determined to be 0.33 at 234 nm and 0.30 at 267 nm. The small relative quantum yields of Br^* indicate that the Br fragments are the main product of the photodissociation. By fitting translational energy distribution of photofragment and comparing the areas of the distribution curves, the Br or Br^* fraction of each channel to the total was obtained and listed in Table 1.

3 Discussion

It is well known that the photodissociation mechanism of aryl halides is very complicated, because there are more electrons and electronic states involved. The electronic transitions usually take place at the C—X (X=Cl, Br, I) bond and/or the C—C π bonds of the benzene ring. The photon energy and the properties of the potential energy surface (PES) will determine what kind of transitions would take place and to which excited states the molecule would be excited. Bersohn and coworkers[11,12,46] have studied the photodissociation of some aryl halides and their experimental results indicated that predissociation was dominant over direct dissociation. However, the direct dissociation and predissociation may exist at the same time and the photodissociation process might have two dissociation channels which compete with each other. Zewail and coworkers[47,48] systemically investigated the photodissociation of iodides by femtosecond laser and time-resolved mass spectrometry. They indicated that the photodissociation of simple molecules, such as iodine, cyanogen iodide, and methyl iodide, is direct dissociation. However, they found the photodissociation of iodobenzene has two dynamical channels: one is direct-mode dissociation due to repulsive (n, σ^*) excitation in the C—I bond and the other is a complex-mode which is electronic predissociation arising from the intramolecular vibrational energy redistribution (IVR) in the benzene ring due to bound (π, π^*) benzene-ring excitation.

Han and coworkers[32] have measured ultraviolet-visible (UV-Vis) absorption spectrum of *o*-bromotoluene, the absorption band of 250–285 nm, usually corresponding to the transition (π, π^*) and/or (n, π^*); they[20] also suggest that there are two different dissociation mechanisms for *o*-bromotoluene: one is a fast dissociation, in which a combination of $\sigma^* \leftarrow n$ transition and the quick intersystem crossing from the singlet excited (π, π^*) state to the triplet (π, σ^*) state is proposed for the dissociation mechanism; the other occurs *via* a hot molecular mechanism. Liu *et al.*[33] calculated potential energy curves of low-lying states using MS-CASPT2. The dissociation products with spin-orbit-coupled states of Br^* and Br were identified by the MS-CASPT2 method in conjunction with spin-orbit interaction through complete ac tive space state interaction (MS-CASPT2/CASSI-SO) calculations. They indicate that the photon initially excites *o*-bromotoluene to the first (π, π^*) singlet state S_1 at 266 nm and the experimentally observed fast and slow channels were assigned, respectively, to (i) the predissociation of the repulsive (n, σ^*) triplet state T_4 after ISC from the initially excited state S_1, or the predissociation of the repulsive (n, σ^*) singlet state S_2 after internal conversion (IC) from the initially excited S_1 state, and (ii) dissociation *via* the hot molecule mechanism after the IC from the originally excited S_1 state. At 266 nm, the photodissociation of *o*-bromotoluene mainly generates ground product Br.

In our experiment results, the branching ratios of the ground state $\mathrm{Br}(^2P_{3/2})$ and spin-orbit excited state $\mathrm{Br}^*(^2P_{1/2})$ have been de-

termined by selecting particular wavelength in REMPI. The total relative quantum yield Φ(Br) was determined to be 0.70 at 267 nm. That is consistent with *ab initio* calculation results[33]. The higher vibrational level of S_1 is excited at 234 nm compared with that at 267 nm; however the photodissociation mechanism at 234 and 267 nm is still same. The relative quantum yield Φ(Br) is still the main component at 234 nm. From the energy curves[33], it is easy to understand that the fast channels come from predissociation between the S_1 (π, π^*) state and the repulsive (n, σ^*) states. But photodissociation mechanism of the slow channels needs further illustration.

Considering the expression of the anisotropy parameter β[49,50]:

$$\beta=2\frac{1+\omega^2\tau^2}{1+4\omega^2\tau^2}P_2(\cos\chi) \quad (10)$$

where ω is the angular velocity of the parent molecule, τ is the dissociation lifetime. $P_2(\cos\chi)$ is the second order Legendre polynomial, and χ is the angle between the transition moment and the direction of the photofragment. If the molecule dissociates instantaneously on absorption of a photon and the kinetic energy of dissociation is very large in comparison with the energy of rotation, then the parameter β is given by a simple equation:

$$\beta=2P_2(\cos\chi) \quad (11)$$

where χ is the angle between the electric transition dipole moment and the direction of dissociation. Eq.(11) is based on the assumption that the molecule is nonrotating. In the general case, the molecule is rotating, then two sorts of effects occur, both of which diminish the β value[49]. First, the dissociation may not be instantaneous, i.e., the excited molecule may be in a metastable state with an average lifetime before dissociation. Second, when the molecule does at last dissociate, the velocity of separation may be sufficiently low that the molecule rotates appreciably during the dissociation. The β values of the slow channels are about 0.1, and the angular distributions of the dissociation fragments are nearly isotropic. The β values are diminished due to the very hot molecule mechanism. The highly excited vibration levels of S_0 (hot molecule, denoted as S_0^*) is populated by internal conversion from S_1 state, then the dissociation occurs slowly. The molecule is rotating when *o*-bromotoluene dissociates slowly, and thus the angular distributions will be nearly isotropic. The fraction f_{tr} is about 0.1, which means that 90% of the available energy is partitioned into the fragment internal energy. After dissociation, the fragments of *o*-bromotoluene are still very hot. Based on the above discussion, we confirmed that the slow channels occur *via* the hot molecular mechanism.

4 Conclusions

The photodissociation dynamics of *o*-bromotoluene has been investigated at 234 and 267 nm using velocity map imaging combined with REMPI technique. The velocity distributions mostly can be fitted with two Gaussian curves. The fast one corresponds to the predissociation from the excited $S_1(\pi, \pi^*)$ state to the repulsive (n, σ^*) state. The slow one corresponds to dissociation *via* the hot molecule mechanism, after IC from the originally excited S_1 state to high vibrationally excited level of the S_0 state. From the relative quantum yields, the ground-state Br($^2P_{3/2}$) is the main product in the photolysis of *o*-bromotoluene at 234 and 267 nm. Because of the hot molecule mechanism, the photodissociation products of slow channels are nearly isotropic. The photodissociation products of fast channels are more anisotropic.

References

1 Johnson, B. R.; Kittrell, C.; Kelly, P. B.; Kinsey, J. L. *J. Phys. Chem.*, **1996, 100**: 7743

2 Philips, D. L.; Lawrence, B. A.; Valentini, J. J. *J. Phys. Chem.*, **1991, 95**: 9085

3 Rattigan, O. V.; Shallcross, D. E.; Cox, R. A. *J. Chem. Soc. Faraday Trans.*, **1997, 93**: 2839

4 Eppink, A. T. J. B.; Parker, D. H. *J. Chem. Phys.*, **1999, 110**: 832

5 Xu, H.; Guo, Y.; Liu, S.; Ma, X.; Dai, D.; Sha, G. *J. Chem. Phys.*, **2002, 117**: 5722

6 Wu, G.; Jiang, B.; Ran, Q.; Zhang, J.; Harich, S. A.; Yang, X. *J. Chem. Phys.*, **2004, 120**: 2193

7 Amatatsu, Y.; Yabushita, S.; Morokuma, K. *J. Chem. Phys.*, **1996, 104**: 9783

8 Samartzis, P. C.; Bakker, B. L.; Parker, D. H.; Kitsopoulos, T. N. *J. Phys. Chem. A*, **1999, 103**: 6106

9 Tang, Y.; Ji, L.; Zhu, R.; Wei, Z.; Zhang, B. *ChemPhysChem*, **2005, 6**: 2137

10 Tang, Y.; Lee, W. B.; Hu, Z.; Zhang, B.; Lin, K. C. *J. Chem. Phys.*, **2007, 126**: 064302

11 Dzvonik, M.; Yang, S. C.; Bersohn, R. *J. Chem. Phys.*, **1974, 61**: 4408

12 Freedman, A.; Yang, S. C.; Kawasaki, M.; Bersohn, R. *J. Chem. Phys.*, **1980, 72**: 1028

13 Ichimura, T.; Mori, Y.; Shinohara, H.; Nishi, N. *Chem. Phys. Lett.*, **1986, 125**: 263

14 Ichimura, T.; Mori, Y.; Shinohara, H.; Nishi, N. *J. Chem. Phys.*, **1997, 107**: 835

15 Hwang, H. J.; El-Sayed, M. A. *J. Chem. Phys.*, **1992, 96**: 856

16 Kadi, M.; Ivarsson, E.; Davidsson, J. *Chem. Phys. Lett.*, **2004, 384**: 35

17 Kadi, M.; Davidsson, J. *Chem. Phys. Lett.*, **2003, 378**: 172

18 Liu, Y. J.; Persson, P.; Karlsson, H. O.; Lunell, S.; Kadi, M.; Karlsson, D.; Davidsson, J. *J. Chem. Phys.*, **2004, 120**: 6502

19 Zhang, H.; Zhu, R. S.; Wang, G. J.; Han, K. L.; He, G. Z.; Lou, N. Q. *J. Chem. Phys.*, **1999, 110**: 2922

20 Zhu, R. S.; Zhang, H.; Wang, G. J.; Gu, X. B.; Han, K. L.; He, G. Z.; Lou, N. Q. *Chem. Phys. Lett.*, **1999, 313**: 98

21 Ichimura, T.; Mori, Y.; Shinohara, H.; Nishi, N. *Chem. Phys.*, **1994, 189**: 117

22 Kadi, M.; Davidsson, J.; Tarnovsky, A. N.; Rasmusson, M.; Akesson, E. *Chem. Phys. Lett.*, **2001, 350**: 93

23 Pence, W. H.; Baughcum, S. L.; Leone, S. R. *J. Phys. Chem.*, **1985, 85**: 3844

24 Freitas, J. E.; Hwang, H. J.; El-Sayed, M. A. *J. Phys. Chem.*, **1995, 99**: 7395

25 Griffiths, J. A.; Junk, K.; El-Sayed, M. A. *J. Phys. Chem.*, **1996, 100**: 7989

26 Liu, Y. J.; Persson, P.; Lunell, S. *J. Phys. Chem. A*, **2004, 108**: 2339

27 Huang, C. L.; Jiang, J. C.; Mebel, A. M.; Lee, Y. T.; Ni, C. K. *J. Am. Chem. Soc.*, **2003, 125**: 9814

28 Lee, S. H.; Wu, C. Y.; Yang, S. K.; Lee, Y. P. *J. Chem. Phys.*, **2006, 125**: 144301

29 Zhu, R. S.; Zhang, H.; Wang, G. J.; Gu, X. B.; Han, K. L.; He, G. Z.; Lou, N. Q. *Chem. Phys.*, **1999, 248**: 285

30 Borg, O. A.; Liu, Y. J.; Persson, P.; Lunell, S.; Karlsson, D.; Kadi, M.; Davidsson, J. *J. Phys. Chem. A*, **2006, 110**: 7045

31 Zhang, H.; Zhu, R. S.; Wang, G. J.; Han, K. L.; He, G. Z.; Lou, N. Q. *Chem. Phys. Lett.*, **1999, 300**: 483

32 Gu, X. B.; Wang, G. J.; Huang, J. H.; Han, K. L.; He, G. Z.; Lou, N. Q. *Chem. Phys.*, **2003, 287**: 285

33 Liu, Y. J.; Tian, Y. C.; Fang, W. H. *J. Chem. Phys.*, **2008, 128**: 064307

34 Unny, S.; Du, Y.; Zhu, L.; Truhins, K.; Gordan, R. J.; Sugita, A.; Kawasaki, M.; Matsumi, Y.; Delmdahl, R.; Parker, D. H.; Berces, A. *J. Phys. Chem. A*, **2001, 105**: 2270

35 Poulsen, M. D.; Skovsen, E.; Stapelfeldt, H. *J. Chem. Phys.*, **2002, 117**: 2097

36 Peronne, E.; Poulsen, M. D.; Stapelfeldt, H.; Bisgaard, C. Z.; Hamilton, E.; Seideman, T. *Phys. Rev. A*, **2004, 70**: 063410

37 Tang, Y.; Lee, W. B.; Zhang, B.; Lin, K. C. *J. Phys. Chem. A*, **2008, 112**: 1421

38 Zhang, F.; Cao, Z. Z.; Qin, X.; Liu, Y. Z.; Wang, Y. M.; Zhang, B. *Acta Phys. -Chim. Sin.*, **2008, 24**(8): 1335 [张 锋, 曹振洲, 覃 晓, 刘玉柱, 王艳梅, 张 冰. 物理化学学报, **2008, 24**(8): 1335]

39 Chen, Y.; Zhang, C. H.; Cao, Z. Z.; Zhang, B. *Acta Phys. -Chim. Sin.*, **2008, 24**(5): 844 [陈 荫, 张昌华, 曹振洲, 张 冰. 物理化学学报, **2008, 24**(5): 844]

40 Zhang, S.; Wang, Y.; Tang, B. F.; Zheng, Q.; Zhang, B. *Chem. Phys. Lett.*, **2005, 413**: 129

41 Tang, Y.; Ji, L.; Tang, B. F.; Zhu, R. S.; Zhang, S.; Zhang, B. *Acta Phys. -Chim. Sin.*, **2004**, **20**(4): 344 [唐 颖, 姬 磊, 唐碧峰, 朱荣淑, 张 嵩, 张 冰. 物理化学学报, **2004**, **20**(4): 344]

42 Weast, R. C. Handbook of chemisty and physics. Cleveland, OH: CRC Press, 1972: 300–305

43 Benson, S. W. Thermochemical kinetics. New York: Wiley, 1968: 78–82

44 Zare, R. N.; Herschbach, D. R. *Proc. IEEE.*, **1963, 51**: 173

45 Zare, R. N. *Mol. Photochem.*, **1972, 4**: 1

46 Kawasaki, M.; Lee, S. J.; Bersohn, R. *J. Chem. Phys.*, **1977, 66**: 2647

47 Zhong, D. P.; Zewail, A. H. *J. Phys. Chem. A*, **1998, 102**: 4031

48 Cheng, P. Y.; Zhong, D.; Zewail, A. H. *Chem. Phys. Lett.*, **1995, 237**: 399

49 Yang, S.; Bersohn, R. *J. Chem. Phys.*, **1974, 61**: 4400

50 Inoue, G.; Kawasaki, M.; Szto, H.; Kikuchi, T.; Kobayashi, S.; Arikawa, T. *J. Chem. Phys.*, **1987, 87**: 722